Received: 22 August 2023 | Revised: 19 September 2023 | Accepted: 22 September 2023

DOI: 10.1002/pol.20230615

RESEARCH ARTICLE

JOURNAL OF POLYMER SCIENCE WILEY

Versatile synthesis of siloxane-based graft copolymers with tunable grafting density

Colton A. D'Ambra[1] | **Michael Czuczola**[2] | **Patrick T. Getty**[1] | **Elizabeth A. Murphy**[2] | **Allison Abdilla**[2,3] | **Souvagya Biswas**[4] | **Jodi M. Mecca**[3] | **Thomas D. Bekemeier**[4] | **Steven Swier**[3] | **Craig J. Hawker**[1,2,5] | **Christopher M. Bates**[1,2,5,6]

[1]Materials Department, University of California, Santa Barbara, California, USA

[2]Department of Chemistry and Biochemistry, University of California, Santa Barbara, California, USA

[3]Dow Performance Silicones, Dow, Auburn, Michigan, USA

[4]Core R&D, Dow, Midland, Michigan, USA

[5]Materials Research Laboratory, University of California, Santa Barbara, California, USA

[6]Department of Chemical Engineering, University of California, Santa Barbara, California, USA

Correspondence
Craig J. Hawker and Christopher M. Bates, Materials Department, University of California, Santa Barbara, CA 93106, USA.
Email: hawker@mrl.ucsb.edu and cbates@ucsb.edu

Funding information
Division of Materials Research, Grant/Award Numbers: 2308708, 1933487, 1844987

Abstract

A versatile synthetic platform is reported that affords high molecular weight graft copolymers containing polydimethylsiloxane (PDMS) backbones and vinyl-based polymer side chains with excellent control over molecular weight and grafting density. The synthetic approach leverages thiol-ene click chemistry to attach an atom-transfer radical polymerization (ATRP) initiator to a variety of commercially available poly(dimethylsiloxane-*co*-methylvinylsiloxane) backbones (PDMS-*co*-PVMS), followed by controlled radical polymerization with a wide scope of vinyl monomers. Selective degradation of the siloxane backbone with tetrabutylammonium fluoride confirmed the controlled nature of side-chain growth via ATRP, yielding targeted side-chain lengths for copolymers containing up to 50% grafting density and overall molecular weights in excess of 1 MDa. In addition, by using a mixture of thiols, grafting density and functionality can be further controlled by tuning initiator loading along the backbone. For example, solid-state fluorescence of the graft copolymers was achieved by incorporating a thiol-containing fluorophore along the siloxane backbone during the thiol-ene click reaction. This simple synthetic platform provides facile control over the properties of a wide variety of grafted copolymers containing flexible PDMS backbones and vinyl polymer side chains.

KEYWORDS

ATRP, graft copolymers, high molecular weight, PDMS, PMMA

1 | INTRODUCTION

Graft copolymers are a useful class of advanced materials with properties that can be precisely tuned by modifying the backbone and side chains.[1–5] Numerous experimental and computational studies have yielded insights into how these design parameters influence material properties,[6–11] leading to applications in viscosity modification,[12,13] thermoplastic elastomers,[14–19] photonics,[20–22] pressure sensors,[23] 3D printing,[24,25] and polymer composites.[26–28]

The development of this diverse range of graft-copolymer-based materials has been enabled by controlled

polymerization techniques along with grafting-to,[29–36] grafting-through,[37–40] or grafting-from[41–50] methodologies to attach the requisite side chains. The grafting-from method, in combination with atom-transfer radical polymerization (ATRP), is of particular interest due to the broad range of vinyl-based polymer side chains that can be synthesized from a initiator-functionalized parent backbone. Key to this versatility is the compatibility and stability of the ATRP process towards siloxanes.[40,51–54] The resulting graft copolymers with siloxane backbones are broadly desirable because of the unique properties imparted by flexible and thermally stable Si—O—Si bonds.[55–57]

Several research groups have reported the synthesis of graft copolymers with siloxane backbones using controlled radical polymerization.[58–60] However, these studies are limited to low grafting densities and modest backbone molecular weights due to the prevalence of radical-radical coupling reactions that lead to crosslinked gels.[61] Despite these limitations, researchers have developed unique applications for graft copolymers with siloxane backbones including water-repellant pigment dispersants and thermally stable liquid-crystalline polymers.[62,63] A versatile synthetic platform that provides access to a wider range of PDMS graft copolymers with high molecular weights and tunable grafting densities would therefore provide unique access to libraries of PDMS-based materials for identifying novel structure–property relationships, bridging the gap between linear block copolymers and polymeric bottlebrushes.

Herein, we report the development of a versatile methodology for preparing PDMS-based graft copolymer libraries with tunable molecular weights and grafting densities (Scheme 1). This strategy leverages robust thiol-ene click chemistry to quantitatively functionalize commercially available polydimethylsiloxane-*co*-polyvinylmethylsiloxane (PDMS-*co*-PVMS) with thiol-containing ATRP initiators. Subsequent chain growth of methyl methacrylate (MMA) and styrene (S) was performed using copper(I)-catalyzed ATRP, yielding graft copolymers with tunable molecular weights and grafting densities as evidenced by selective degradation experiments. Numerous polyacrylate grafts were prepared using copper(II)-catalyzed, UV-light-induced ATRP to demonstrate the broad applicability of this approach to a wide variety of graft copolymers and polymerization conditions. This synthetic strategy enables the preparation of high molecular weight materials (>1 MDa) with versatility further illustrated through the incorporation of mixed thiols during PDMS backbone functionalization. In summary, the methodology described herein provides access to an expanded library of PDMS-based graft copolymers and highlights the potential to readily manipulate material properties like solid-state fluorescence.

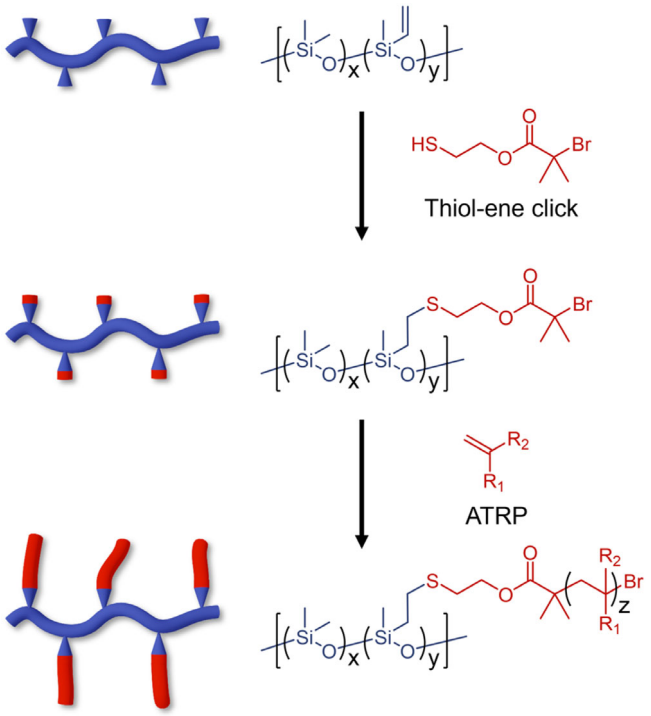

SCHEME 1 General synthetic strategy for preparing siloxane-based macroinitiators and corresponding graft copolymers.

2 | RESULTS AND DISCUSSION

In designing a versatile synthetic strategy, PDMS-*co*-PVMS copolymers were selected as starting materials given the wide range of molecular weights and levels of backbone functionalization that are commercially available. PVMS content was determined using ^{1}H NMR by comparing the integration values of the unique methyl resonances for dimethylsiloxane repeat units at $\delta = 0$–0.3 ppm to the integration values for the distinct vinyl protons from vinylmethylsiloxane repeat units at $\delta = 5.7$–6.1 ppm. For thiol-ene coupling, 2-mercaptoethyl α-bromoisobutyrate (HS–EBiB) was synthesized by acylation of bis(2-hydroxyethyl)disulfide followed by reduction of the disulfide to give the desired thiol group (Schemes S1 and S2, Figures S1 and S4). Quantitative functionalization was achieved for PDMS-*co*-PVMS copolymers ranging from 17 to 225 kDa and a wide range of grafting densities (1–50 mol% PVMS incorporation, Scheme S3, and Figure S5). For the initial library of PMMA graft copolymers, polymeric side chains were grown from the siloxane backbone through copper(I) ATRP using CuBr as the catalyst and *N*,*N*,*N*′,*N*″,*N*″-pentamethyldiethylenetriamine (PMDETA) as ligand in chlorobenzene (Scheme S5). This reaction sequence affords a range of samples denoted PDMS$_x$-g$_y$-PMMA$_z$ where x refers to the PDMS backbone molecular weight (in Da), y represents the number of grafts, and

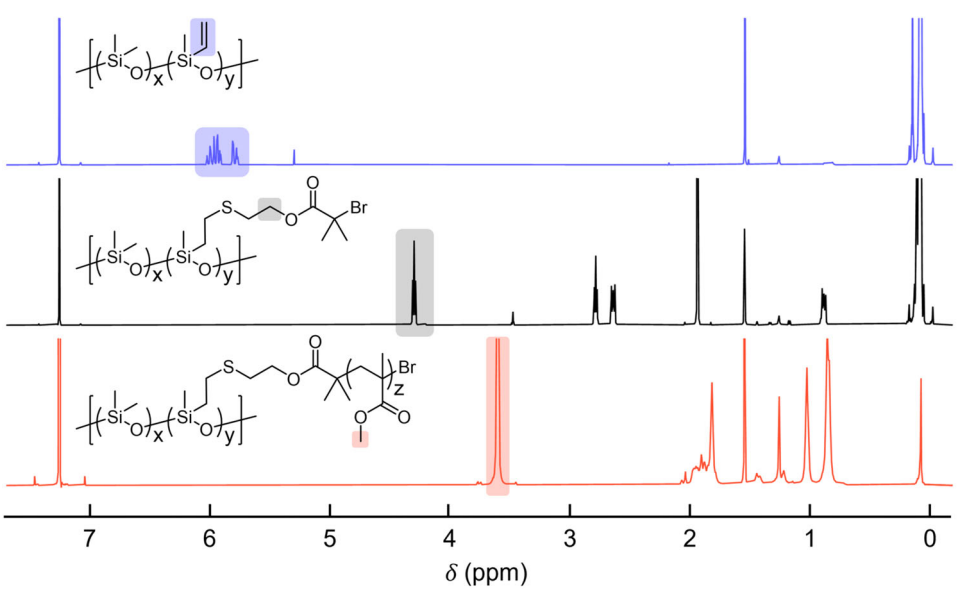

FIGURE 1 Representative ^{1}H NMR characterization of PDMS$_{28k}$-g_{35}-PMMA$_{20k}$ synthesized from PDMS-*co*-PVMS with diagnostic protons highlighted.

z corresponds to the average PMMA molecular weight per graft (in Da). Figure 1 demonstrates the successful synthesis of PDMS macroinitiator and subsequent MMA polymerization to produce PDMS$_{28k}$-g_{35}-PMMA$_{20k}$.

Because highly branched macromolecules like PDMS$_{28k}$-g_{35}-PMMA$_{20k}$ have a significantly smaller hydrodynamic radius compared to linear analogues, ^{1}H NMR spectroscopy proved to be more reliable than size-exclusion chromatography (conventional calibration) for estimating molecular weights. The introduction of PMMA-grafted arms was confirmed using ^{1}H NMR spectroscopy (Figure 1) with the diagnostic resonance of the methyl ester protons of the MMA repeat units observed at $\delta = 3.6$ ppm. Furthermore, the H atoms corresponding to —CH_2 and —CH_3 units along the PMMA backbone are present at $\delta = 1.7$–2.1 ppm and $\delta = 0.7$–1.1 ppm, respectively (Figure S6). To calculate the total PMMA molecular weight, the ratio of ^{1}H NMR integration values for the methyl ester group from PMMA to the methyl groups along the siloxane backbone was calculated with the assumption that the molecular weight of the siloxane backbone remained constant. For the graft copolymer PDMS$_{28k}$-g_{35}-PMMA$_{20k}$, the ratio of MMA to DMS protons was 8.5:1 which leads to a total calculated molecular weight of ~700 kDa. The side-chain molecular weight was determined assuming equivalent reactivity of each ATRP initiating unit, resulting in an average 20 kDa per PMMA grafted arm.

Size-exclusion-chromatography (SEC) with a differential refractive index (dRI) detector was used to investigate changes in nominal molecular weight and molar mass distribution upon functionalization of PDMS-*co*-PVMS with HS–EBiB and subsequent polymerization of MMA (Figure 2). After attaching the ATRP initiator, the SEC peak

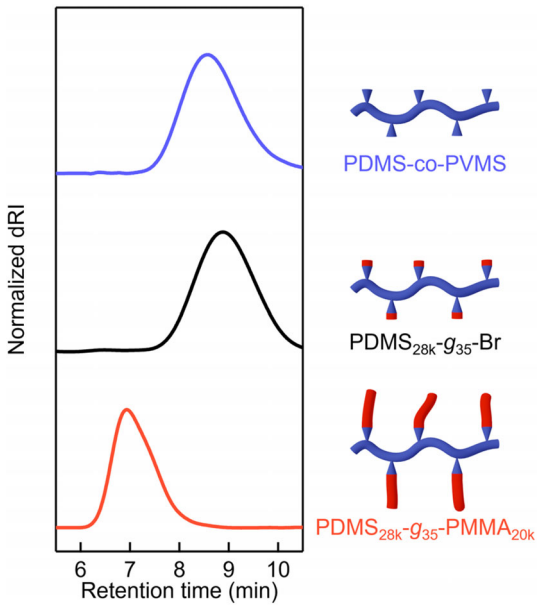

FIGURE 2 SEC traces of PDMS-*co*-PVMS (28 kDa, 35 vinyl units) starting polymer, macroinitiator PDMS$_{28k}$-g_{35}-Br, and graft copolymer PDMS$_{28k}$-g_{35}-PMMA$_{20k}$. The dRI signal for PDMS-*co*-PVMS and PDMS$_{28k}$-g_{35}-Br are inverted for better comparison.

shifts slightly to a higher elution time due to the addition of sterically bulky, polar substituents along the siloxane backbone that lead to a minor reduction in hydrodynamic volume. Upon polymerizing MMA, the SEC peak for the grafted product was observed at significantly lower retention time, confirming the successful grafting-from polymerization of MMA with minimal to no formation of linear homopolymer chains (Figures 2 and S21–S28).

Radical–radical coupling that leads to crosslinking is a known challenge in grafting-from strategies, frequently

resulting in insoluble gels due to bimolecular termination of propagating polymer chains.[64] This is especially significant for graft copolymers with a high number of initiation sites along the backbone where even minimal radical–radical coupling can form a network. For example, traditional conditions were only successful for low molecular weight copolymers with up to 35 grafts,[65] and insoluble gels were obtained for samples having higher levels of backbone functionalization at conversions as low as 15%. To address this issue, polymerization conditions were optimized to minimize radical–radical coupling reactions at high grafting densities and molecular weights. Here, by lowering the catalyst and monomer concentrations while increasing reaction temperature, higher conversions were achieved while avoiding gelation allowing for the synthesis of graft copolymers based on a wide variety of PDMS-*co*-PVMS starting polymers featuring both high molecular weights and high degrees of backbone functionalization (Table 1).

To further demonstrate the synthetic versatility of this strategy, styrene and acrylic monomers were also polymerized from the $PDMS_{28k}$-g_{35}-Br macroinitiator. As expected for styrene polymerization at 110 °C, a minor amount of autopolymerization leads to a small peak in the SEC chromatogram that corresponds with polystyrene homopolymer (Figure S29). In contrast, acrylates are readily polymerized via photoinitiated ATRP using copper(II) bromide as catalyst and an aliphatic tertiary amine (Me_6Tren) ligand under 365 nm irradiation (Figure S6). These conditions efficiently polymerize numerous acrylates[66–68] with poly(methyl acrylate) (PMA), poly(oligoethyleneglycol acrylate) (POEGA), poly(isobornyl acrylate) (PiBA), and poly(tetrafluoroethyl acrylate) (PTFEA) successfully grown from the same PDMS macroinitiator, highlighting the ability to incorporate hydrophilic, hydrophobic, and fluorinated repeat units into PDMS-based graft copolymers (Figures S7–S11). Notably, in contrast to MMA, acrylates can be polymerized to higher conversions ~70% without gelation, though the SEC traces showed increased homopolymerization (Figures S29–S34).

After demonstrating the versatility of preparing grafted macromolecules from ATRP-functionalized PDMS backbones, thermal properties of the resulting copolymers were characterized via differential-scanning calorimetry (DSC). In all cases, the DSC profiles were dominated by the vinyl grafts as they constitute most of the mass fraction for each material.[69–71] For example, the DSC trace of macroinitiator $PDMS_{28k}$-g_{35}-Br shows a sharp decrease in heat flow around −110 °C corresponding to the glass-transition temperature (T_g) of PDMS (Figure S35). Following grafting, each copolymer displayed a T_g value corresponding to that expected for a homopolymer of the side chain with values ranging from ~110 °C for PMMA to −70 °C for POEGA. Note that

TABLE 1 Summary of synthesized grafts copolymers.

Sample	Siloxane M_n (kDa)	Number of grafts[a]	Graft M_n (kDa per graft)[a]	Total M_n (kDa)[a]
$PDMS_{17k}$-$g_{2.3}$-$PMMA_{20k}$	17	2.3	20	63
$PDMS_{17k}$-$g_{2.3}$-$PMMA_{41k}$	17	2.3	41	111
$PDMS_{23k}$-$g_{3.3}$-$PMMA_{15k}$	23	3.3	15	73
$PDMS_{28k}$-g_{35}-$PMMA_{20k}$	28	35	20	730
$PDMS_{50k}$-g_{300}-$PMMA_{4k}$	50	300	4	1300
$PDMS_{50k}$-g_{300}-$PMMA_{14k}$	50	300	14	4000
$PDMS_{225k}$-g_{350}-$PMMA_{1k}$	225	350	1	580
$PDMS_{225k}$-g_{350}-$PMMA_{5k}$	225	350	5	2000
$PDMS_{225k}$-g_{350}-$PMMA_{17k}$	225	350	17	>5000
$PDMS_{225k}$-g_{350}-$PMMA_{68k}$	225	350	68	>5000
$PDMS_{28k}$-g_{35}-PS_{23k}	28	35	23	830
$PDMS_{28k}$-g_{35}-PMA_{17k}	28	35	17	620
$PDMS_{225k}$-g_{350}-PMA_{22k}	225	350	22	>5000
$PDMS_{225k}$-g_{350}-PMA_{65k}	225	350	65	>5000
$PDMS_{28k}$-g_{35}-$PiBA_{40k}$	28	35	40	1400
$PDMS_{28k}$-g_{35}-$PTFEA_{18k}$	28	35	18	660
$PDMS_{28k}$-g_{35}-$POEGA_{20k}$	28	35	20	730

[a]Calculated based on ^{1}H NMR.

these materials conceivably could still contain a T_g corresponding to PDMS that is just much weaker, broader, and difficult to detect due to the high weight percent of acrylate repeat units. Additionally, POEGA grafted systems exhibited a cold crystallization at −45 °C and a melting peak at −5 °C (Figure S36).

To verify the controlled nature of grafting-from polymerizations, graft copolymers were treated with tetrabutylammonium fluoride (TBAF) to selectively degrade the PDMS backbone (Scheme S7). The resulting homopolymer side-chains were isolated by precipitation (for high molecular weights) or by washing with water for low-molecular-weight materials. Figure 3 highlights degradation results for $PDMS_{28k}$-g_{35}-$PMMA_{20k}$ which illustrate minimal chain–chain coupling during the ATRP process. The symmetrical SEC trace measured after degradation corresponds to a molecular weight of 24 kDa with a molar-mass dispersity of $Đ = 1.18$ relative to poly(methyl methacrylate) standards. This compares favorably with the theoretical molecular weight of 20 kDa based on the original grafted copolymer and PDMS backbone. Likewise, most graft copolymers in this study contain side chains with actual molecular weights agreeing closely with theoretical values (Table 2). Notably, these observations suggest that the bimodal character of some SEC traces after graft growth (e.g., Figures S21 and S22) originates from a confluence of dispersity in the number of arms per molecule and molar mass, not an uncontrolled graft polymerization process. Only at very high grafting density was deviation between the observed grafted and theoretical molecular weights detected, which may be due to incomplete initiation, although low dispersities were again observed (Figures S37–S49). These selective degradation studies support the well-controlled nature of the graft polymerization process with minimal radical–

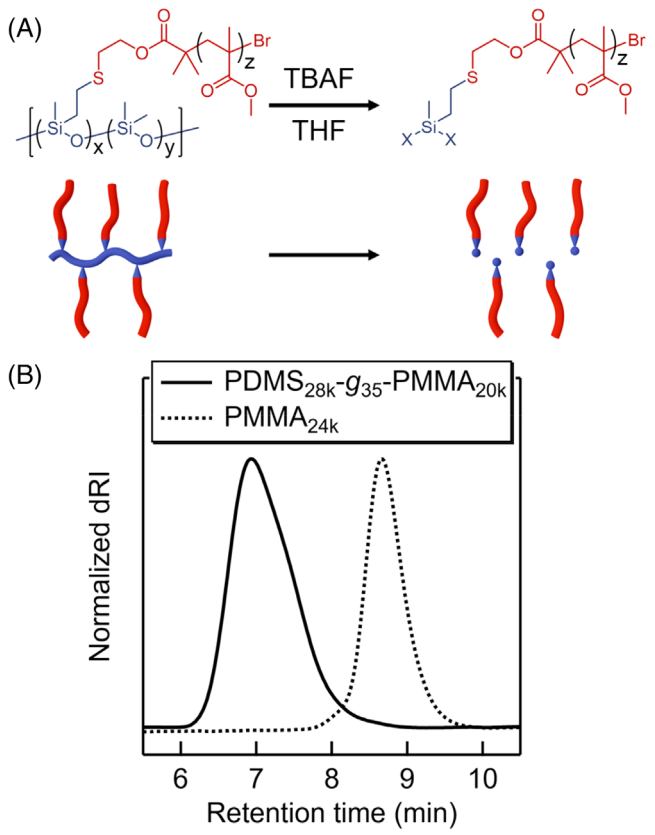

FIGURE 3 (A) Selective backbone degradation of PDMS-based graft copolymers with TBAF permits characterization of the side chains after grafting-from polymerization. (B) SEC traces corresponding to $PDMS_{28k}$-g_{35}-$PMMA_{20k}$ and recovered $PMMA_{24k}$ with a measured number-average molecular weight of 24 kDa (PMMA standards).

TABLE 2 Molecular weight and dispersity of isolated grafted side-chains following degradation of the PDMS backbone with TBAF.

Sample	Calculated side-chain M_n (kDa)[a]	Homopolymer M_n (kDa)[b]	$Đ$
$PDMS_{17k}$-$g_{2.3}$-$PMMA_{21k}$	21	33	1.31
$PDMS_{28k}$-g_{35}-$PMMA_{20k}$	20	24	1.18
$PDMS_{50k}$-g_{300}-$PMMA_{4k}$	4	4	1.30
$PDMS_{50k}$-g_{300}-$PMMA_{14k}$	14	26	1.32
$PDMS_{225k}$-g_{350}-$PMMA_{1k}$	1	3	1.31
$PDMS_{225k}$-g_{350}-$PMMA_{5k}$	5	8	1.39
$PDMS_{225k}$-g_{350}-$PMMA_{17k}$	17	21	1.17
$PDMS_{225k}$-g_{350}-$PMMA_{68k}$	68	67	1.36
$PDMS_{28k}$-g_{35}-PS_{23k}	23	25	1.20
$PDMS_{28k}$-g_{35}-PMA_{17k}	17	16	1.19
$PDMS_{225k}$-g_{350}-PMA_{22k}	22	20	1.15
$PDMS_{225k}$-g_{350}-PMA_{65k}	65	43	1.36
$PDMS_{28k}$-g_{35}-$PiBA_{40k}$	40	23	1.10

[a]Calculated based on ^{1}H NMR.
[b]SEC molecular weights compared to linear PMMA standards for PMMA and to linear PS samples for PS, PMA, and PiBA.

radical coupling even at high molecular weights and high grafting densities.

An advantage of this synthetic platform is the ability to introduce a mixture of functionalized and unfunctionalized thiols along the PDMS backbone. For example, grafting density was tuned by functionalizing a single parent PDMS-*co*-PVMS copolymer with mixtures of the thiol-functionalized ATRP initiator (HS–EBiB) and 1-dodecanethiol (DDSH) as a non-functional diluent. As illustrated in Scheme 2, a library of materials with different grafting densities was achieved by changing the molar ratio of HS–EBiB to DDSH from 1:9 to 1:4 and 2:3 during the thiol-ene coupling step. In this case, the starting PDMS-*co*-PVMS copolymer had a molecular weight of 225 kDa with an average of 350 vinyl functional groups along the backbone.

For this library of materials, the ratio of substituents along the backbone was determined by ^{1}H NMR spectroscopy (Figures S50–S52) with the incorporation of functionalized and unfunctionalized thiols quantified by integrating the unique resonances at $\delta = 2.7$ ppm and $\delta = 2.5$ ppm corresponding to the two S—CH_2 units of the ATRP initiator fragment and the two S—CH_2 units of the dodecyl substituent, respectively (Figure 4). In all cases, the product composition corresponded closely with the feed ratio. Additionally, unique resonances at 4.3 ppm corresponding to the ATRP initiator are present and integrate to the expected values. By simply varying the relative ratio of EBiB and DDSH, three macroinitiators were synthesized from the same commercially available 225 kDa PDMS-*co*-PVMS polymer to produce macroinitiators with approximately 35, 80, and 140 ATRP initiation sites per chain (out of a possible 350 vinyl groups). As shown in Figure S53, the SEC traces of these macroinitiators exhibit a monotonic increase in retention time with increasing EBiB functionalization that is fully consistent with the shift described above for $PDMS_{28k}$-g_{35}-Br. PMMA side chains with a target molecular weight of 20 kDa were grafted from each of the PDMS macroinitiators in this sequence using optimized ATRP conditions: 0.25:1 molar ratio of CuBr to PMDETA and a 4:1 volume ratio of chlorobenzene to monomer at 70 °C. After purification of the graft copolymers, ^{1}H NMR spectroscopy was used to determine overall copolymer composition with molecular weights measured to be ~3 MDa, 1.6 MDa, and 840 kDa based on 140, 80, and 35 grafted arms, respectively. As expected, the SEC traces in Figure 5A show a decrease in retention time as the number of grafts increases due to the increase in overall molecular weight. The siloxane backbone was then selectively degraded using TBAF with the isolated grafted arms being analyzed by SEC (Figure 5B). Significantly, the grafted arms from the three different starting copolymers were shown to have monomodal molecular weight distributions with low dispersities of ~1.2 and similar

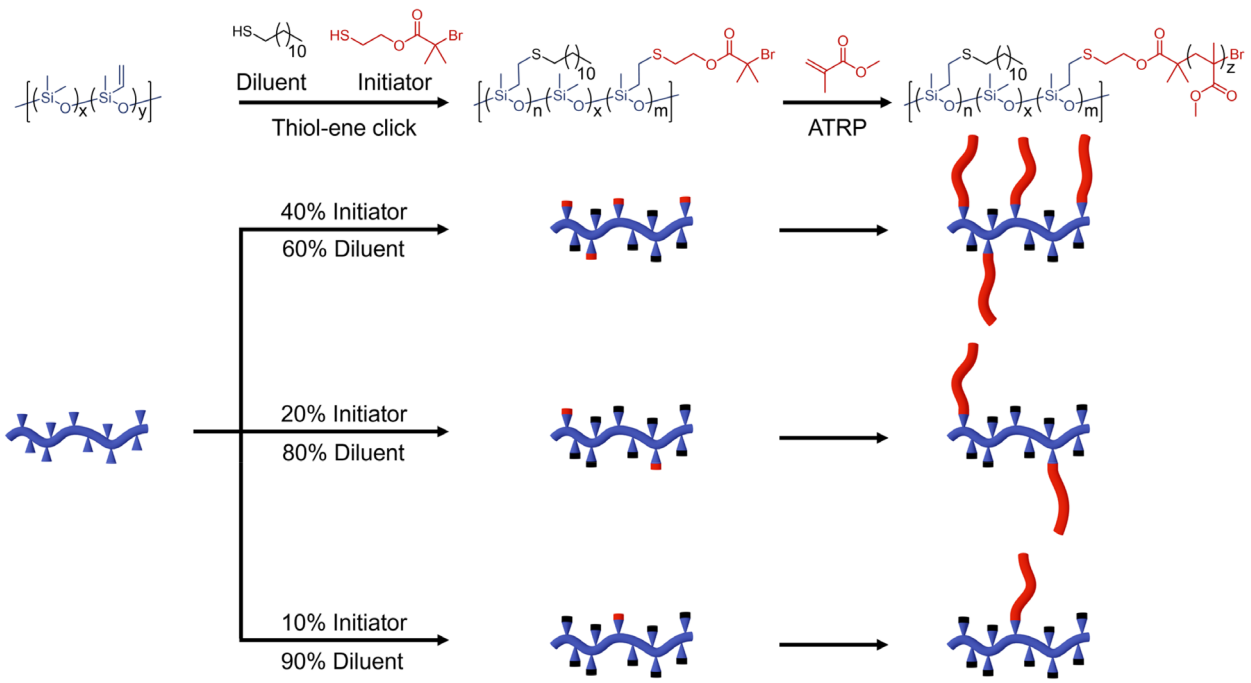

SCHEME 2 Synthesis of PDMS macroinitiator with a tunable number of ATRP initiation sites by varying the ratio of HS–EBiB to DDSH using the same starting PDMS-*co*-PVMS copolymer.

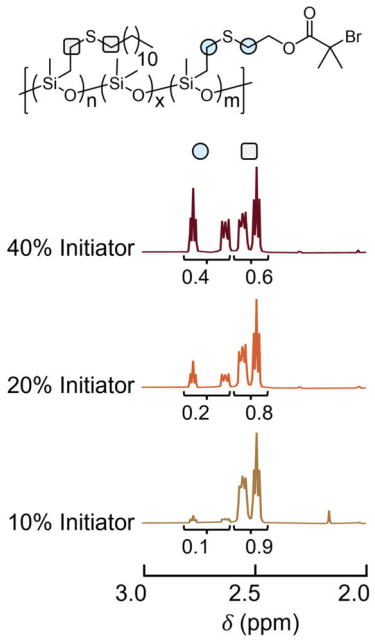

FIGURE 4 ^{1}H NMR spectra for PDMS macroinitiators with the thioether peaks of each substituent labeled and quantified to show the ratio of functional EBiB units to non-functional DDSH groups. The resulting macroinitiators have 140, 80, and 35 ATRP initiation groups along the backbone and were synthesized from the same starting materials by varying the ratio of thiols.

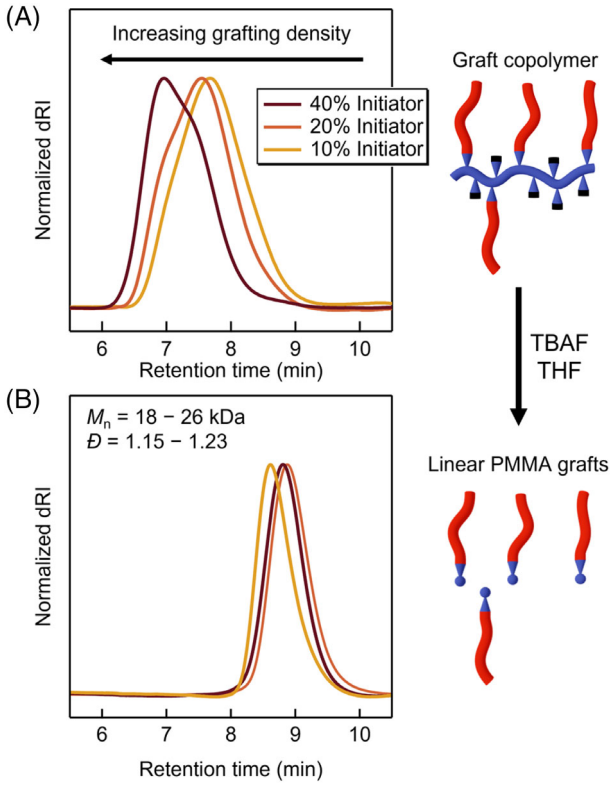

FIGURE 5 (A) SEC traces of graft copolymers with tunable grafting density and controlled molecular weights starting from the same commercially available vinyl siloxane. (B) Recovered linear PMMA grafts after selective degradation of the graft copolymer with TBAF.

molecular weights based on PMMA standards (∼20 kDa). The similarity in growth profiles for the grafting process illustrates the ability to tune molecular weight and grafting density with vinyl-based grafts based on a commercially available, high molecular weight PDMS starting polymer.

To further highlight the ability to introduce different thiols, a mixture of EBiB and a thiol-containing fluorophore was attached to a PDMS backbone (Figure 6A). Due to the overlapping absorbance of 2,2-dimethoxy-2-phenylacetophenone (DMPA) and the fluorophore, the thiol-ene click reaction was performed under thermal conditions using azoisobutyronitrile (AIBN). A molar ratio of 95:5 HS–EBiB:7-mercapto-4-methylcoumain was employed during thiol-ene coupling with ^{1}H NMR spectroscopy again confirming the incorporation of 4-methylcoumarin units (Figure S57). In this system, unique resonances of the methylcoumarin unit were observed for the thioether peak ($\delta = 3.1$ ppm) as well as the methyl unit ($\delta = 2.3$ ppm) and aromatic group ($\delta = 6.2$, 7.1, and 7.4 ppm). Based on the integration of these resonances and those from EBIB, the molar incorporation of fluorophore was calculated to be 4%, which compares favorably with the 5% feed ratio (Figure S58). Further verification of fluorophore incorporation was obtained by SEC analysis using a combination of photodiode array (PDA) and dRI detection (Figure S59), illustrating the consistent level of chromophore incorporation across the molecular weight distribution of the PDMS backbone (Figure S60).

Growth of PMMA chains from the coumarin functionalized PDMS backbone was accomplished using a ratio of 0.25:1 CuBr to ATRP initiator and a 4:1 volume ratio of solvent to monomer at 70 °C. By ^{1}H NMR analysis, the grafted copolymer was shown to have a total molecular weight of ∼300 kDa with ∼8 kDa PMMA grafted arms. Both PDA and dRI detectors attached to an SEC show a shift to lower retention time, corresponding to an increase in molecular weight (Figures S60–S62). As expected, the graft PMMA-PDMS copolymer with covalently bound fluorescent coumarin along its backbone exhibits a strong absorbance at 330 nm while the corresponding graft copolymer with no fluorophore incorporation shows no absorbance (Figure 6B) leading to a significant difference in solid-state fluorescence (Figure 6C).

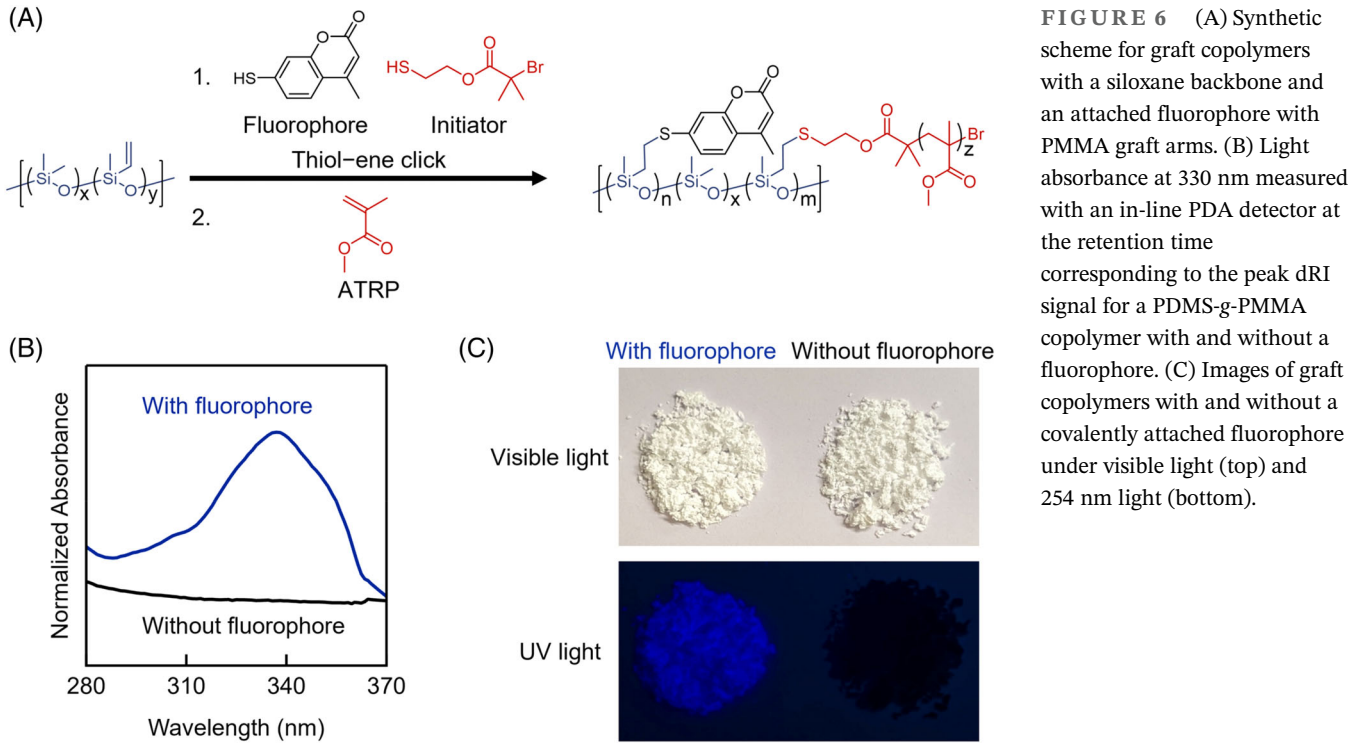

FIGURE 6 (A) Synthetic scheme for graft copolymers with a siloxane backbone and an attached fluorophore with PMMA graft arms. (B) Light absorbance at 330 nm measured with an in-line PDA detector at the retention time corresponding to the peak dRI signal for a PDMS-*g*-PMMA copolymer with and without a fluorophore. (C) Images of graft copolymers with and without a covalently attached fluorophore under visible light (top) and 254 nm light (bottom).

3 | CONCLUSIONS

In summary, a tunable synthetic platform is presented for the preparation of high molecular weight PDMS-*g*-PMMA graft copolymers from commercially available PDMS-*co*-PVMS backbones. Numerous vinyl groups along the backbone were quantitatively functionalized with HS–EBiB using thiol-ene click chemistry followed by the polymerization of a wide range of vinyl monomers using ATRP. This allows grafted arms with good control over molecular weight and low dispersities to be prepared. Importantly, selective backbone degradation enabled the isolation and characterization of linear grafted arms, further highlighting the degree of control over the ATRP process and minimal radical–radical chain coupling even at high molecular weights and high degrees of backbone functionalization. The versatility of this strategy was further exemplified using mixtures of thiols during the initial thiol-ene functionalization step. A combination of EBiB and dodecane thiol (DDSH) as a non-functional thiol allowed for accurate control over the number of ATRP initiation sites per siloxane backbone and tuning of grafting density from a common starting PDMS derivative. Alternatively, a mixture of EBiB and thiol-functionalized fluorophore was used for the synthesis of multifunctional graft copolymers exhibiting solid-state fluorescence due to selective labeling of the PDMS backbone. Based on commercially available starting materials, the versatility and scalability of this synthetic strategy will enable future studies on graft copolymer systems with vinyl polymer side-chains and flexible siloxane-based backbones.

ACKNOWLEDGMENTS

The authors thank Professors Rachel A. Segalman and Glenn H. Fredrickson for intellectual discussions, Dr. Hongjun Zhou for help with NMR experiments, and Dr. Rachel Behrens for assistance with SEC and DSC characterization.

FUNDING INFORMATION

The research reported here was primarily supported by the National Science Foundation Materials Research Science and Engineering Center (MRSEC) at UC Santa Barbara (DMR-2308708, IRG-1, Christopher M. Bates and Craig J. Hawker, synthesis), DMR-1844987 (Christopher M. Bates, characterization), and the BioPACIFIC Materials Innovation Platform of the National Science Foundation under Award No. DMR-1933487 (Christopher M. Bates and Craig J. Hawker, equipment and characterization). The research reported here made use of shared facilities of the UC Santa Barbara MRSEC (NSF DMR-2308708), a member of the Materials Research Facilities Network (www.mrfn.org). This research was also supported by Dow Chemical Company through the Dow Materials Institute at UCSB.

CONFLICT OF INTEREST STATEMENT

The authors declare no competing financial interest.

DATA AVAILABILITY STATEMENT

The data that support the findings of this study are available in the supplementary material of this article. Tabulated data corresponding to all figures in the main text and supplementary information are available free of charge at https://doi.org/10.5061/dryad.5tb2rbp9v.

ORCID

Colton A. D'Ambra https://orcid.org/0000-0002-2837-2901
Craig J. Hawker https://orcid.org/0000-0001-9951-851X
Christopher M. Bates https://orcid.org/0000-0003-0113-2593

REFERENCES

[1] M. W. Matsen, *Macromolecules* **2012**, *45*(4), 2161.
[2] A. E. Levi, J. Lequieu, J. D. Horne, M. W. Bates, J. M. Ren, K. T. Delaney, G. H. Fredrickson, C. M. Bates, *Macromolecules* **2019**, *52*(4), 1794.
[3] M. J. Allen, K. Wangkanont, R. T. Raines, L. L. Kiessling, *Macromolecules* **2009**, *42*(12), 4023.
[4] A. B. Chang, T. P. Lin, N. B. Thompson, S. X. Luo, A. L. Liberman-Martin, H. Y. Chen, B. Lee, R. H. Grubbs, *J. Am. Chem. Soc.* **2017**, *139*(48), 17683.
[5] A. Zografos, N. A. Lynd, F. S. Bates, M. A. Hillmyer, *ACS Macro Lett.* **2021**, *10*(12), 1622.
[6] N. Hadjichristidis, H. Iatrou, M. Pitsikalis, J. Mays, *Prog. Polym. Sci.* **2006**, *31*(12), 1068.
[7] S. Ohno, K. Matyjaszewski, *J. Polym. Sci. Part A: Polym. Chem.* **2006**, *44*(19), 5454.
[8] C. J. Hawker, D. Mecerreyes, E. Elce, J. Dao, J. L. Hedrick, I. Barakat, P. Dubois, R. Jérôme, W. Volksen, *Macromol. Chem. Phys.* **1997**, *198*(1), 155.
[9] J. Paturej, S. S. Sheiko, S. Panyukov, M. Rubinstein, *Sci. Adv.* **2016**, *2*(11), e1601478.
[10] H. Liang, Z. Cao, Z. Wang, S. S. Sheiko, A. V. Dobrynin, *Macromolecules* **2017**, *50*(8), 3430.
[11] K. L. Wooley, C. J. Hawker, J. M. J. Frechet, *Angew. Chem. Int. Ed. Engl.* **1994**, *33*, 82.
[12] M. T. Savoji, D. Zhao, R. J. Muisener, K. Schimossek, K. Schoeller, T. P. Lodge, M. A. Hillmyer, *Ind. Eng. Chem. Res.* **2018**, *57*(6), 1840.
[13] P. Brant, J. Lu, M. Shivokhin, S. Yakovlev, S. Kang, B. Welke, M. Raney, J. Throckmorton, J. Rapp, H. Wang, D. Yablon, *Macromolecules* **2020**, *53*(15), 6353.
[14] W. Wang, W. Lu, A. Goodwin, H. Wang, P. Yin, N. G. Kang, K. Hong, J. W. Mays, *Prog. Polym. Sci.* **2019**, *95*, 1.
[15] N. A. Lynd, F. T. Oyerokun, D. L. O'Donoghue, D. L. Handlin, G. H. Fredrickson, *Macromolecules* **2010**, *43*(7), 3479.
[16] J. Zhang, D. K. Schneiderman, T. Li, M. A. Hillmyer, F. S. Bates, *Macromolecules* **2016**, *49*(23), 9108.
[17] J. Zhang, T. Li, A. M. Mannion, D. K. Schneiderman, M. A. Hillmyer, F. S. Bates, *ACS Macro Lett.* **2016**, *5*(3), 407.
[18] C. Lu, J. Yu, C. Wang, J. Wang, F. Chu, *Carbohydr. Polym.* **2018**, *188*, 128.
[19] F. Jiang, Z. Wang, Y. Qiao, Z. Wang, C. Tang, *Macromolecules* **2013**, *46*(12), 4772.
[20] A. L. Liberman-Martin, C. K. Chu, R. H. Grubbs, *Macromol. Rapid Commun.* **2017**, *38*(13), 1700058.
[21] Z. Wang, C. L. C. Chan, T. H. Zhao, R. M. Parker, S. Vignolini, *Adv. Opt. Mater.* **2021**, *9*(21), 2100519.
[22] T. Kerr-Phillips, M. Damavandi, L. I. Pilkington, K. A. Whitehead, J. Travas-Sejdic, D. Barker, *Polymer* **2022**, *14*(14), 2767.
[23] V. G. Reynolds, S. Mukherjee, R. Xie, A. E. Levi, A. Atassi, T. Uchiyama, H. Wang, M. L. Chabinyc, C. M. Bates, *Mater. Horiz.* **2020**, *7*(1), 181.
[24] S. Nian, J. Zhu, H. Zhang, Z. Gong, G. Freychet, M. Zhernenkov, B. Xu, L. H. Cai, *Chem. Mater.* **2021**, *33*(7), 2436.
[25] R. Xie, S. Mukherjee, A. E. Levi, V. G. Reynolds, H. Wang, M. L. Chabinyc, C. M. Bates, *Sci. Adv.* **2020**, *6*(46), eabc6900.
[26] J. L. Self, A. J. Zervoudakis, X. Peng, W. R. Lenart, C. W. Macosko, C. J. Ellison, *JACS Au* **2022**, *2*(2), 310.
[27] I. Fortelný, J. Jůza, *Materials* **2021**, *14*(24), 7786.
[28] K. Klimovica, S. Pan, T. W. Lin, X. Peng, C. J. Ellison, A. M. Lapointe, F. S. Bates, G. W. Coates, *ACS Macro Lett.* **2020**, *9*(8), 1161.
[29] R. Sarkar, E. B. Gowd, S. Ramakrishnan, *Polym. Chem.* **2020**, *11*(25), 4143.
[30] N. Hadjichristidis, M. Pitsikalis, S. Pispas, H. Iatrou, *Chem. Rev.* **2001**, *101*(12), 3747.
[31] R. Riva, S. Schmeits, C. Jérôme, R. Jérôme, P. Lecomte, *Macromolecules* **2007**, *40*(4), 796.
[32] J. Huang, Z. Xiao, H. Liang, J. Lu, *Polym. Int.* **2014**, *63*(6), 1122.
[33] B. A. Turowec, E. R. Gillies, *Polym. Int.* **2017**, *66*(1), 42.
[34] S. Karamdoust, P. Crewdson, M. Ingratta, E. R. Gillies, *Polym. Int.* **2015**, *64*(5), 611.
[35] S. Karamdoust, C. V. Bonduelle, R. C. Amos, B. A. Turowec, S. Guo, L. Ferrari, E. R. Gillies, *J. Polym. Sci. Part A: Polym. Chem.* **2013**, *51*(16), 3383.
[36] A. Soleimani, M. M. A. R. Moustafa, A. Borecki, E. R. Gillies, *Can. J. Chem.* **2015**, *93*(4), 399.
[37] M. Higuchi, A. Kanazawa, S. Aoshima, *Macromolecules* **2020**, *53*(10), 3822.
[38] T. P. Lin, A. B. Chang, H. Y. Chen, A. L. Liberman-Martin, C. M. Bates, M. J. Voegtle, C. A. Bauer, R. H. Grubbs, *J. Am. Chem. Soc.* **2017**, *139*(10), 3896.
[39] W. Wang, W. Wang, X. Lu, S. Bobade, J. Chen, N. G. Kang, Q. Zhang, J. Mays, *Macromolecules* **2014**, *47*(21), 7284.
[40] Z. Wang, L. Yuan, C. Tang, *Acc. Chem. Res.* **2017**, *50*(7), 1762.
[41] S. Dadashi-Silab, S. Doran, Y. Yagci, *Chem. Rev.* **2016**, *116*(17), 10212.
[42] K. Matyjaszewski, *Adv. Mater.* **2018**, *30*(23), 1706441.
[43] T. Maharana, S. Pattanaik, A. Routaray, N. Nath, A. K. Sutar, *React. Funct. Polym.* **2015**, *93*, 47.
[44] M. K. Thakur, V. K. Thakur, R. K. Gupta, A. Pappu, *ACS Sustain. Chem. Eng.* **2016**, *4*(1), 1.
[45] P. Baek, L. Voorhaar, D. Barker, J. Travas-Sejdic, *Acc. Chem. Res.* **2018**, *51*(7), 1581.
[46] X. Guo, B. Choi, A. Feng, S. H. Thang, *Macromol. Rapid Commun.* **2018**, *39*(20), 1800479.
[47] B. S. Sumerlin, D. Neugebauer, K. Matyjaszewski, *Macromolecules* **2005**, *38*(3), 702.
[48] Z. Wang, Z. Wang, Y. Zhang, F. Jiang, H. Fang, *Polym. Chem.* **2014**, *5*(10), 3379.

[49] M. Wang, S. Kee, P. Baek, M. S. Ting, Z. Zujovic, D. Barker, J. Travas-Sejdic, *Polym. Chem.* **2019**, *10*(46), 6278.
[50] M. Damavandi, P. Baek, L. I. Pilkington, O. Javed Chaudhary, P. Burn, J. Travas-Sejdic, D. Barker, *Eur. Polym. J.* **2017**, *89*, 263.
[51] G. Polymeropoulos, G. Zapsas, K. Ntetsikas, P. Bilalis, Y. Gnanou, N. Hadjichristidis, *Macromolecules* **2017**, *50*(4), 1253.
[52] L. T. Strover, J. Malmström, J. Travas-Sejdic, *Chem. Rec.* **2016**, *16*(1), 393.
[53] J. Coudane, H. Van Den Berghe, J. Mouton, X. Garric, B. Nottelet, *Molecules* **2022**, *27*(13), 4135.
[54] C. Feng, Y. Li, D. Yang, J. Hu, X. Zhang, X. Huang, *Chem. Soc. Rev.* **2011**, *40*(3), 1282.
[55] F. Weinhold, R. West, *Organometallics* **2011**, *30*(21), 5815.
[56] S. J. Clarson, J. J. Fitzgerald, M. J. Owen, S. D. Smith Eds., Silicones and Silicone-Modified Materials, 1st ed., American Chemical Society, Washington, DC **2000**.
[57] E. Berthier, E. W. K. Young, D. Beebe, *Lab Chip* **2012**, *12*(7), 1224.
[58] E. Pouget, J. Tonnar, P. Lucas, P. Lacroix-Desmazes, F. Ganachaud, B. Boutevin, *Chem. Rev.* **2010**, *110*(3), 1233.
[59] Y. Nakagawa, P. J. Miller, K. Matyjaszewski, *Polymer* **1998**, *39*(21), 5163.
[60] E. Taran, B. Donose, K. Higashitani, A. D. Asandei, D. Scutaru, N. Hurduc, *Eur. Polym. J.* **2006**, *42*(1), 119.
[61] F. Seidi, H. Salimi, A. A. Shamsabadi, M. Shabanian, *Prog. Polym. Sci.* **2018**, *76*, 1.
[62] C. Huang, L. Yi, H. Yuan, C. Chen, *Adv. Mater. Res.* **2012**, *441*, 478.
[63] G. Wang, Y. Xiong, H. Tang, *J. Organomet. Chem.* **2015**, *775*, 50.
[64] S. C. Hong, T. Pakula, K. Matyjaszewski, *Macromol. Chem. Phys.* **2001**, *202*(17), 3392.
[65] L. Y. Shi, Y. Zhou, Z. Shen, X. H. Fan, *Macromolecules* **2012**, *45*(13), 5530.
[66] A. E. Levi, L. Fu, J. Lequieu, J. D. Horne, J. Blankenship, S. Mukherjee, T. Zhang, G. H. Fredrickson, W. R. Gutekunst, C. M. Bates, *Macromolecules* **2020**, *53*(2), 702.
[67] E. A. Murphy, Y. Q. Chen, K. Albanese, J. R. Blankenship, A. Abdilla, M. W. Bates, C. Zhang, C. M. Bates, C. J. Hawker, *Macromolecules* **2022**, *55*(19), 8875.
[68] A. Anastasaki, V. Nikolaou, Q. Zhang, J. Burns, S. R. Samanta, C. Waldron, A. J. Haddleton, R. McHale, D. Fox, V. Percec, P. Wilson, D. M. Haddleton, *J. Am. Chem. Soc.* **2014**, *136*(3), 1141.
[69] H. Lin, E. van Wagner, J. S. Swinnea, B. D. Freeman, S. J. Pas, A. J. Hill, S. Kalakkunnath, D. S. Kalika, *J. Membr. Sci.* **2006**, *276*(1–2), 145.
[70] A. M. Granville, S. G. Boyes, B. Akgun, M. D. Foster, W. J. Brittain, *Macromolecules* **2005**, *38*(8), 3263.
[71] W. Jakubowski, A. Juhari, A. Best, K. Koynov, T. Pakula, K. Matyjaszewski, *Polymer* **2008**, *49*(6), 1567.

SUPPORTING INFORMATION

Additional supporting information can be found online in the Supporting Information section at the end of this article.

How to cite this article: C. A. D'Ambra, M. Czuczola, P. T. Getty, E. A. Murphy, A. Abdilla, S. Biswas, J. M. Mecca, T. D. Bekemeier, S. Swier, C. J. Hawker, C. M. Bates, *J. Polym. Sci.* **2023**, 1. https://doi.org/10.1002/pol.20230615